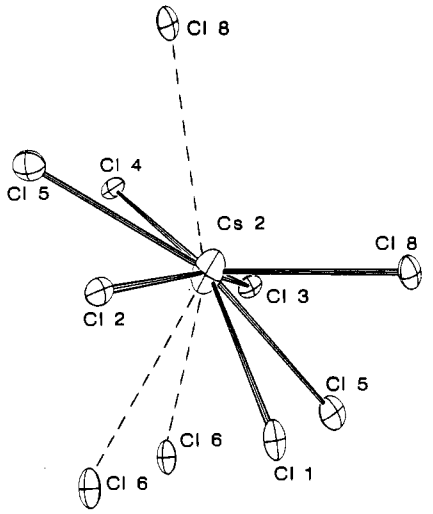

Figure 7. Cs(2) site in $Cs_3Zr_6Cl_{16}C$, which shows a remarkable similarity to the Cs(1) site (Figure 6). Dashed lines indicate distances over 3.90 Å (50% ellipsoids).

the full occupancy of the smaller Cs(1) site. The phase is probably nonstoichiometric in this respect. Changing the interstitial to beryllium presumably provides a full occupancy of cation sites in the phase $Cs_4Zr_6Cl_{16}Be$ that was also synthesized.

Surprisingly, the rather unusual chlorine environment around both of the cesium atoms appears to affect their thermal parameters only slightly, such that both are somewhat elongated in the direction perpendicular to the "Cl_6 ring" (~2:1) (compare $CsKZr_6Cl_{15}B$[14]).

The $Cs_3Zr_6Cl_{16}C$ structure and hence that of $Na_4Zr_6Cl_{16}Be$ show an unmistakable similarity to the structure of $K_3Zr_6Cl_{15}Be$.[15] The puckered square netlike sheets of $Zr_6Cl_{12}Z$ clusters found in the last beryllide are clearly evident lying perpendicular to $\vec{a}$ in Figure 7 in ref 15. The linear Cl^{a-a} bridges that link these layers in $\vec{a}$ have disappeared in $Cs_3Zr_6Cl_{16}C$ as a result of the addition of another chlorine atom to each cluster. The cluster layers in the new cesium phase have also been translated half a unit cell in the $\vec{b}$ and $\vec{c}$ directions with respect to one another to make room for the additional chlorine atoms and have opened up slightly, reducing the cluster tilt. The $(\vec{b} + \vec{c})/2$ translation of the cluster layers with respect to one another may also be thought of as a reflection of every other layer through a mirror plane lying in the cluster layer. The end result in either case is the same; i.e., every cluster layer is puckered in the same direction at the same time. The relationship between the cation sites in the two structure types is considerably less clear because of the layer translation.

The layerlike structures of $Na_4Zr_6Cl_{16}Be$ and $Cs_3Zr_6Cl_{16}C$ offer an opportunity to pursue an intercalation/ion-exchange chemistry similar to that of the more common layered MX_2 compounds.[25] The flexibility of the cluster sheets that can be achieved through rotation and bending of the $Zr-Cl^{a-a}-Zr$ bonds should allow many differently sized and shaped monoatomic and polyatomic cations to be accommodated. Oxidation or reduction of the $Zr_6Cl_{12}Z$ clusters under mild conditions may also be possible. Two exploratory ion-exchange reactions of $Na_4Zr_6Cl_{16}Be$ with $KAlCl_4$ and $CsAlCl_4$ at 300 and 400 °C, respectively, appear encouraging in that reactions occurred in both cases judging from powder patterns of the products. Unfortunately, the flexibility of cluster sheets that makes them attractive host materials also makes indexing and interpretation of the powder diffraction patterns difficult because of the large intensity and line position changes associated with the puckering of the cluster sheets. Thus far, neither ion-exchange product has been characterized further.

The phase $Na_4Zr_6Cl_{16}Be$ also shows hints of what may be an interesting solution chemistry. It dissolves in acetone to give a dark red-violet solution that becomes colorless in air within minutes with the formation of a white precipitate. Further study will be required to determine if the chemistry can be controlled or is of interest.

Acknowledgment. We are indebted to Professor R. A. Jacobson for the continued provision of diffraction and computing facilities. This research was supported by the National Science Foundation, Solid State Chemistry, via Grant DMR-8318616, and was carried out in facilities of Ames Laboratory, DOE. R.P.Z. was also the holder of Departmental Gilman and Procter and Gamble Fellowships.

Supplementary Material Available: Tables of anisotropic thermal parameters for $Na_4Zr_6Cl_{16}Be$ and $Cs_3Zr_6Cl_{16}C$ and crystallographic details (3 pages); a listing of the observed and calculated structure factor data for the same compounds (12 pages). Ordering information is given on any current masthead page.

(25) Rouxel, J. *Intercalated Layered Materials*; Levy, F., Ed.; D. Riedel Publishing Co.: Dordrecht, The Netherlands, 1979; pp 201-250.

Contribution from the Departments of Chemistry, Iowa State University, Ames, Iowa 50011, and Texas A&M University, College Station, Texas 77843

Encapsulation of Heavy Transition Metals in Iodide Clusters. Synthesis, Structure, and Bonding of the Unusual Cluster Phase $Y_6I_{10}Ru$

Timothy Hughbanks[1a] and John D. Corbett*,[1b]

Received August 19, 1988

The reaction of Y_3Ru with YI_3 at 800-950 °C in a sealed Ta container affords $Y_7I_{12}Ru$ and $Y_6I_{10}Ru$, the yield of the latter increasing with time or temperature. $Y_7I_{12}Ru$ is isostructural with $Sc_7Cl_{12}B$ on the basis of Guinier powder data ($R\bar{3}$, $Z = 3$, $a = 15.4373$ (7) Å, $c = 10.6126$ (6) Å). The new structure type of $Y_6I_{10}Ru$ was deduced from its lattice dimensions and symmetry and was refined with single-crystal X-ray diffraction data ($P\bar{1}$, $Z = 1$; $a = 9.456$ (2) Å, $b = 9.643$ (2) Å, $c = 7.629$ (1) Å, $\alpha = 97.20$ (2)°, $\beta = 105.04$ (2)°, $\gamma = 107.79$ (2)°; $R = 5.2$, $R_w = 6.7\%$ for 1421 independent reflections, $2\theta \leq 55°$, Mo Kα radiation). The structure consists of Y_6I_{12} clusters centered by Ru and condensed into infinite chains through sharing of inner iodine (I^i) atoms with the two adjoining clusters, viz., $Y_6I^i_8I^{i-i}_{4/2}Ru$. The clusters are connected in the other two directions through the more typical I^{i-a} linkages at metal vertices. The nominal octahedral Y_6Ru cluster shows a 0.21-Å tetragonal *compression*, contrary to the usual behavior of ML_6 units with a t_{1u}^4 HOMO. Charge-iterative extended Hückel calculations show that the distortion originates with Y-Y interactions because of a negligible participation of the high-lying Ru 5p orbitals in the HOMO.

Introduction

A remarkable feature of metal halide clusters composed of the electron-poorer transition metals such as zirconium and the rare-earth elements is that all M_6X_{12}-type clusters appear to *require* an interstitial heteroatom Z within. The interstitial atom in this role provides both additional bonding electrons and orbitals for the formation of strong M-Z bonds within the cluster. Although zirconium chloride clusters are the more versatile struc-

(1) (a) Texas A&M University. (b) Iowa State University.

0020-1669/89/1328-0631$01.50/0

turally,[2] the zirconium iodide analogues have proven to be notably more adaptable in the range of interstitials that can be incorporated. The main-group elements B, C, Al, Si, P, and Ge have all been encapsulated in Zr_6I_{12} or Zr_6I_{14} cluster compositions that contain about 14 cluster-based electrons.[3-5] Even more surprising is the stability of analogous phases in which the transition metals chromium through cobalt are bound within the same types of clusters, favorable electron counts now being in the neighborhood of 18 because of the addition of the nonbonding e_g^4 orbitals on the interstitial.[6,7]

The related interstitial chemistry of rare-earth-metal clusters is less well-defined. Known examples include those with second-period elements within clusters such as $Sc(Sc_6I_{12}(B,C))$,[8] with dicarbon in $Gd_{10}Cl_{18}(C_2)_2$,[9,10] and with monocarbon in condensed cluster chains such as Sc_5Cl_8C[11] and Y_4I_5C.[12] The 3d transition metals again provide comparable examples in $R(R_6I_{12}Z)$ phases, R = Sc, Y, Pr, and Gd (and presumably others) and Z = Mn–Ni, but these are observed to tolerate a wider range of electron counts, 16–19.[13] The R–Z distances in these are found to be notably shorter than in analogous RZ_x intermetallic phases.

Although MO theory has given useful guidance as to the bonding and stability of compounds within a certain range of electron counts, the method does not provide definitive answers regarding whether a particular compound that meets the electronic requirements can be synthesized or will exist. Thus, the possible extension of the array of workable transition-metal interstitials to the 4d and 5d elements requires experimental answers. Our exploratory investigations aimed at synthesizing $R_7I_{12}Ru$ phases not only have succeeded for R = Y (and others) but also have yielded the novel cluster compound $Y_6I_{10}Ru$ that is the principal subject of this article.

Experimental Section

Syntheses. The high quality of the metal used, the synthesis and sublimation of YI_3, reaction techniques utilizing welded and SiO_2-jacketed niobium containers, and Guinier powder diffraction procedures have all been described recently.[11-13] The ruthenium powder employed was from Engelhard Metals. The binary reactant Y_3Ru was prepared by arc-melting the elements under argon; this composition turns out to be more reactive than Ru powder and more convenient as well since the reaction stoichiometry $Y_3Ru + 4YI_3$ is correct for the preparation of $Y_7I_{12}Ru$.

The stoichiometries of the new phases $Y_6I_{10}Ru$ and $Y_7I_{12}Ru$ (= $Y_6I_{10.3}Ru_{0.86}$) are sufficiently close that both may be obtained from the same reaction, particularly since they appear to have different kinetic stabilities. All of the following reactions were loaded for the $Y_7I_{12}Ru$ stoichiometry unless noted otherwise. Reactions of Y_3Ru with YI_3 at 800, 850, or 900 °C for 34, 30, or 17 days, respectively, give good (~80%) yields of $Y_6I_{10}Ru$ plus small amounts of $Y_7I_{12}Ru$ (10–20%), unreacted YI_3 and, sometimes, YOI. Similarly, a reaction of powdered Ru with Y and YI_3 at a high temperature, 1000 °C for 6 days, followed by annealing at 900 °C for 1 day, gives comparable yields with, in this case, some single crystals of the phase of interest that are >0.5 mm in size. On the other hand, reactions utilizing the normal *powdered* Ru as the interstitial source that are run under comparable conditions to the first group above, 875–925 °C for 18–11 days, give 80–100% of the alternative $Y_7I_{12}Ru$, the remainder being mainly $Y_6I_{10}Ru$. Nonetheless, a quantitative yield of $Y_6I_{10}Ru$ is obtained from reactions loaded according to its subsequently determined stoichiometry when one allows 22 days at 950 °C. The foregoing observations suggest that $Y_7I_{12}Ru$ is metastable or marginally stable and that it is best formed at lower temperatures via the slower reactions that take place with bulk Ru during which the activity of YI_3 remains higher. No reduced binary yttrium iodides are known, and omission of Ru from these reactions gives no new products.

Table I. Data Collection and Refinement Parameters for $Y_6I_{10}Ru$[a,b]

space group; Z	$P\bar{1}$; 1
latt dimens	
a, b, c, Å	9.456 (2), 9.643 (2), 7.629 (1)
α, β, γ, deg	97.20 (2), 105.04 (2), 107.79 (2)
V, Å^3	623.7 (2)
abs coeff μ, cm^{-1} (Mo Kα)	268
normalized range of transmission coeff	0.33–1.0
R;[c] R_w[d]	5.2; 6.7

[a] Dimensions from least-squares refinement of Guinier powder diffraction pattern with Si as internal standard; λ = 1.54056 Å. [b] $F_o \geq 3\sigma_F$ and $I_o > 3\sigma_I$. [c] $R = \sum(|F_o| - |F_c|)/\sum|F_o|$. [d] $R_w = [\sum w(|F_o| - |F_c|)^2/\sum w|F_o|^2]^{1/2}$.

X-ray Studies. The compound $Y_7I_{12}Ru$ was easily identified on comparison of its powder pattern with that calculated from the parameters of $Y_7I_{12}Fe$.[13] The lattice constants so derived are a = 15.4373 (7) Å, c = 10.6126 (6) Å, V = 2190.1 Å^3 ($R\bar{3}$, Z = 3). A black well-faceted crystal (dimensions of 0.14 × 0.2 × 0.22 mm) of what turned out to be $Y_6I_{10}Ru$ was mounted on a Syntex diffractometer, and 15 tuned reflections were indexed to a triclinic cell with lattice parameters as follows: a = 9.448 (3) Å, b = 9.633 (4) Å, c = 7.617 (4) Å, α = 97.20 (4)°, β = 105.03 (3)°, γ = 107.78 (3)°, V = 621.6 (5) Å^3. (The Guinier powder pattern generally gives the more accurate values—Table I.) Diffraction data were collected with monochromatized Mo Kα radiation at room temperature for reflections with indices $\pm h,\pm k,\pm l$ and $2\theta < 55°$. The data were empirically corrected for absorption by using the results of three ψ scans at different values of θ, each utilizing the average of Friedel pair data. The structural data were collected by using variable scan speeds (1.0–29.0° min^{-1}); no decay of the intensity of two check reflections was observed. The absorption correction is relatively large (μ = 268 cm^{-1}) since yttrium lies on the absorption edge of Mo Kα radiation, and so ψ-scans were collected at even slower speeds (0.5–0.8° min^{-1}) to improve the statistical significance of the data.

A structural model for $Y_6I_{10}Ru$ was deduced in an intuitive manner. First, a strong clue to the stoichiometry can be obtained from the cell volume. If we assume the new structure is also based on a distorted close-packed array of iodines, then we can calculate the number of iodine atoms per cell using the above cell volume of $Y_7I_{12}Ru$ as a reference. Thus the number of "iodide positions" in the new phases is estimated to be (623.7/730.0) × 13 = 11.11. In writing this equation we use the fact that the interstitial Ru sits on an "iodide position" in $Y_7I_{12}Ru$ and so there are 13 such positions in the rhombohedral cell.[13] Assuming the new phase also contains isolated six-metal atom clusters (the crystal habit suggests that it does not contain condensed cluster chains or sheets), the indicated stoichiometry is $Y_6I_{10}Ru$ in which the Ru atom is assumed once again to sit on an "iodide position" in a close-packed array. If every cluster contains a Ru atom, as expected from experience with all other such compounds, then Z = 1 ($P\bar{1}$), and the interstitial must be at the cell origin.

Further information is given by the lengths of the a and b axes (9.45 and 9.63 Å, respectively), which are close to the rhombohedral axis length for $Y_7I_{12}Ru$ (9.59 Å). In $Y_7I_{12}Ru$, the rhombohedral axes are just the vectors that join centers of adjacent clusters, and their length is determined by the manner in which adjacent clusters fit together via edge-bridging iodines that are exo to metal vertices in another and vice versa.[8] It was therefore concluded that the intercluster linkages in $Y_6I_{10}Ru$ in the (110) section must be essentially identical with those observed for $Y_7I_{12}Ru$ in corresponding view. This conclusion is further bolstered by the fact that the angle between the a and b axes is close to that between the rhombohedral axes in $Y_7I_{12}Ru$, viz., α_R = 107.21° vs γ = 107.78° here.

In order to achieve a $Y_6I_{10}Ru$ stoichiometry, it was clear that the cluster must share edge-bridging iodides of the $Y_6I_{12}Ru$ cluster unit in the third direction to produce $Y_6I_8I_{4/2}Ru$. Furthermore, it seemed likely that each cluster would share two inner iodides with each of the two neighbors situated on either side of it along the c direction. The orientation of these neighboring clusters was deduced by modeling various sharing arrangements and rejecting those arrangements that gave inappropriate c axis lengths, unsuitable β and γ angles, or both. Only the structural model subsequently refined met these conditions.

Refinement proceeded smoothly using the initial positions derived as described above for *all* atoms. The programs and procedures have been referenced before.[14] The largest residual in the final difference map was

(2) Ziebarth, R. P.; Corbett, J. D. *J. Am. Chem. Soc.* **1985**, *107*, 4571.
(3) Smith, J. D.; Corbett, J. D. *J. Am. Chem. Soc.* **1985**, *107*, 5704.
(4) Smith, J. D.; Corbett, J. D. *J. Am. Chem. Soc.* **1986**, *108*, 1927.
(5) Rosenthal, G.; Corbett, J. D. *Inorg. Chem.* **1988**, *27*, 53.
(6) Hughbanks, T.; Rosenthal, G.; Corbett, J. D. *J. Am. Chem. Soc.* **1986**, *108*, 8289.
(7) Hughbanks, T.; Rosenthal, G.; Corbett, J. D. *J. Am. Chem. Soc.* **1988**, *110*, 1511.
(8) Hwu, S.-J.; Corbett, J. D. *J. Solid State Chem.* **1986**, *64*, 331.
(9) Warkentin, E.; Masse, R.; Simon, A. *Z. Anorg. Allg. Chem.* **1982**, *491*, 323.
(10) Simon, A. *J. Solid State Chem.* **1985**, *57*, 2.
(11) Hwu, S.-J.; Dudis, D. S.; Corbett, J. D. *Inorg. Chem.* **1987**, *26*, 469.
(12) Kauzlarich, S. M.; Hughbanks, T.; Corbett, J. D.; Klavins, P.; Shelton, R. N. *Inorg. Chem.* **1988**, *27*, 1791.
(13) Hughbanks, T.; Corbett, J. D. *Inorg. Chem.* **1988**, *27*, 2022.

Table II. Positional Parameters for $Y_6I_{10}Ru$[a]

	x	y	z
Y1	0.0412 (4)	−0.2483 (3)	0.1160 (4)
Y2	0.2756 (4)	0.0814 (3)	−0.0289 (4)
Y3	0.1320 (4)	0.1717 (3)	0.3614 (4)
I1	0.4625 (3)	0.2779 (3)	0.3579 (4)
I2	0.0921 (3)	0.4688 (2)	0.2698 (4)
I3	0.3733 (3)	−0.1815 (3)	0.0881 (4)
I4	−0.1893 (3)	0.0922 (3)	0.4472 (3)
I5	0.2689 (3)	0.3552 (2)	−0.2075 (3)
Ru	0	0	0

[a] Space group $P\bar{1}$; $Z = 1$.

Table III. Important Distances (Å) and Angles (deg) in $Y_6I_{10}Ru$

		Distances	
Y1–Y2	3.763 (4)	Y2–I3[b]	3.327 (4)
Y1–Y2[a]	3.705 (4)	Y2–I4	3.177 (4)
Y1–Y3	3.843 (5)	Y2–I5	3.126 (4)
Y1–Y3[a]	3.969 (4)	Y3–I1	2.983 (4)
Y2–Y3	3.688 (5)	Y3–I2	3.138 (4)
Y2–Y3[a]	3.853 (5)	Y3–I4	3.200 (4)
Y1–Ru	2.752 (3)	Y3–I4	3.156 (4)
Y2–Ru	2.556 (3)	Y3–I5[b]	3.244 (4)
Y3–Ru	2.772 (3)	I3[b]–I1	4.200 (4)[c]
Y1–I2	3.101 (4)	I3[b]–I3	4.182 (6)
Y1–I2[b]	3.215 (4)	I4[b]–I4	4.146 (4)
Y1–I3	3.074 (4)	I5[b]–I5	4.159 (4)
Y1–I4	3.215 (4)	I1–I2	4.185 (5)
Y1–I5	3.087 (4)	I1–I4	4.151 (4)
Y2–I1	3.041 (5)	I1–I5	4.158 (4)
Y2–I3	3.103 (4)	I2–I5	4.198 (4)
		Angles	
Y1–Ru–Y3	91.84 (9)	Ru–Y1–I2	177.5 (1)
Y1–Ru–Y2	90.2 (1)	Ru–Y2–I3	177.3 (1)
Y2–Ru–Y3	87.5 (1)	Ru–Y3–I5	176.0 (1)
I2–Y1–I4	165.6 (1)	Y1–I4–Y3	76.4 (1)
I3–Y1–I5	167.2 (1)	Y1–I4–Y3	96.1 (1)
I1–Y3–I4	168.9 (1)	Y2–I4–Y3	74.9 (1)
I2–Y3–I4	166.6 (1)	Y2–I4–Y3	96.5 (1)
I1–Y2–I4	161.5 (1)	Y3–I4–Y3	92.4 (1)
I3–Y2–I5	160.3 (1)		

[a] Inversion related atom. [b] Exo I^{a-i}. [c] Only I–I distances ≤ 4.20 Å are listed.

<0.8 e/Å^3 and was located about 1 Å from I2. Other parameters are in Table I.

Results and Discussion

$Y_6I_{10}Ru$ Structure. The refined positional parameters in $Y_6I_{10}Ru$ are listed in Table II; thermal parameter and structure factor data are available as supplementary material. Some important distances and angles are listed in Table III.

The new structure type found for $Y_6I_{10}Ru$ is constructed from distorted Y_6I_{12}-type (edge-bridged) clusters centered by ruthenium. As in $Zr_6I_{12}C$[3] and the closely related $Sc(Sc_6Cl_{12}B)$ structures,[8] all terminal positions are occupied by edge-bridging halogens from other clusters. But in this case the iodine content is reduced to $Y_6I_{10}Ru$ through sharing of two inner iodine atoms per cluster with those in adjoining clusters, viz., $Y_6I_8I_{4/2}Ru$.

As was deduced in modeling the solution of this structure (see Experimental Section), the intercluster bonding in (110) sections of $Y_6I_{10}Ru$ is essentially the same as in the $R(R_6X_{12}Z)$ structure. Figure 1 shows four centrosymmetric $Y_6I_{12}Ru$ clusters in $Y_6I_{10}Ru$ that make up an infinite sheet of this character. A similar diagram would apply to the (110) section (or equivalent) in $Y_7I_{12}Ru$ in the rhombohedral setting as well. This portion of the three-dimensional structure is generated through bonding of the edge-sharing atoms I2 and I3 in one cluster as exo atoms at Y1 and Y2 vertices in other clusters, respectively, and vice versa.

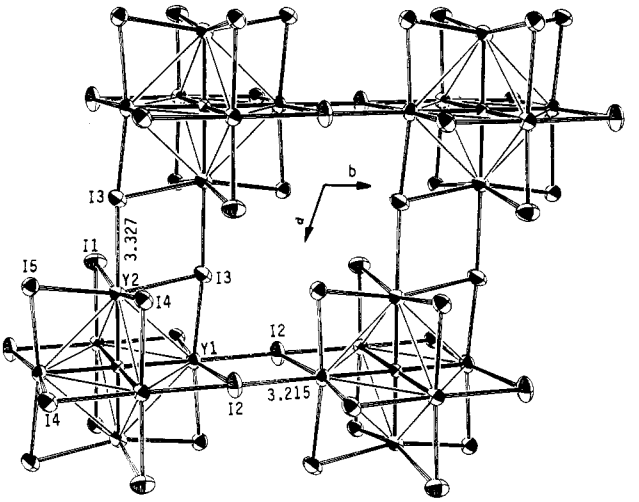

Figure 1. (110) section of $Y_6I_{10}Ru$ with Y–Ru bonds emphasized. Centers of symmetry occur at the Ru and at the midpoint of the rhomboidal intercluster bridges Y1–I2 and Y2–I3 (75% probability thermal ellipsoids).

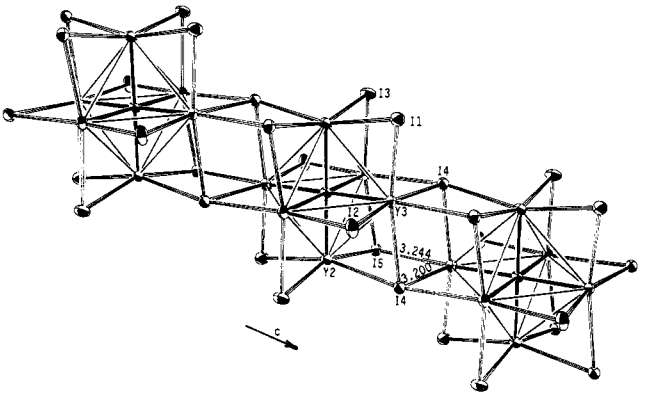

Figure 2. $^1_\infty[Y_6I_{10}Ru]$ chains within $Y_6I_{10}Ru$ that contain the $I4^{i-i}$ and $I5^{i-a}$ linkages. Centers of symmetry occur at Ru and at the midpoint of the I4–Y3 rhomboid. The view is approximately normal to that in Figure 1 (75% ellipsoids).

Figure 2 depicts the way in which these Y_6I_{12} clusters are fused to form $^1_\infty[Y_6I_{10}Ru]$ chains along the *a* axis; Figure 1 may then be thought of as a cross-sectional slice of four of these interconnected chains. As can be seen from inspection of the central cluster in Figure 2, each cluster in the chain has four edge-bridging inner iodides that are common with the two adjacent clusters, namely, the I4 atoms that bridge both Y2–Y3 edges in one cluster and Y1–Y3 sides in its nearest neighbor. Finally, pairs of the neighboring I5 atoms simultaneously occupy exo positions on Y3 vertices in adjoining clusters along the chain in a parallel manner and in a bonding mode analogous to that seen in Figure 1.

The four-coordinate $I4^{i-i}$ atoms appropriately show the longest $Y-I^i$ distances, 3.19 Å on average, while two-coordinate $I2^i$ atoms at the other extreme are only edge bridging and have the shortest Y–I bonds, 3.01 Å on average. Three-coordinate I2, I3, and $I5^{i-a}$ distances to yttrium average an intermediate 3.10 Å. The $Y-I^{a-i}$ (exo) bonds as a group are the longest in the structure; those trans to the short Y2–Ru bonds within the cluster (see below) are the longest (3.33 Å), probably because of closed-shell contacts that I3 makes with the adjoining edge-bridging iodines, while those iodides bound trans to the longer Y3–Ru and Y1–Ru bonds are closer (3.22 and 3.24 Å).

The linking of clusters into chains through the $I4^{i-i}$ construction accompanied by the parallel $I5^{i-a}$ bonding, Figure 2, is quite similar to that encountered in the phase $Sc_6I_{11}C_2$.[15] The latter involves clusters that have been elongated by about 25% along a pseudo-4-fold axis in order to accommodate a dicarbon interstitial,

(14) Hwu, S.-J.; Corbett, J. D.; Poeppelmeier, K. R. *J. Solid State Chem.* **1985**, *57*, 43.

(15) Dudis, D. S.; Corbett, J. D. *Inorg. Chem.* **1987**, *26*, 1933.

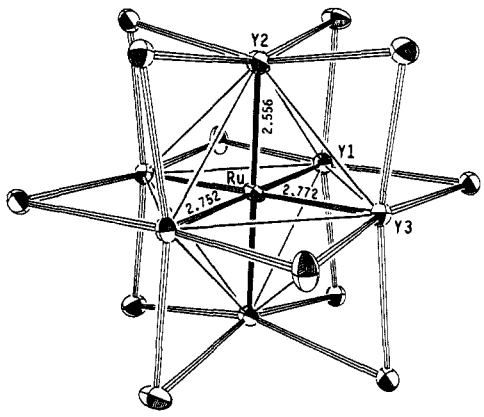

Figure 3. $Y_6I_{12}Ru$ cluster within $Y_6I_{10}Ru$ showing Y–Ru distances (75% ellipsoids).

and the different stoichiometry is analogously achieved by linking only pairs of clusters together with inner iodines that are common to two clusters. The relative Sc–I distances among the four different iodine functions in that phase are comparable to those found here except for those that reflect the substantial distortion of the $Sc_6(C_2)$ framework. Simon[10] has reported the condensation of $Gd_{10}I_{18}(C_2)_2$ double clusters into $^1_\infty[Gd_{10}I_{16}(C_2)_2]$ chains in which iodides are shared between adjacent double clusters in an entirely analogous fashion.

The most interesting feature of the $Y_6I_{10}Ru$ structure is the ruthenium-centered cluster. This characteristic pertains not only because the compound represents the heaviest interstitial of any kind reported to bond in a heterometal cluster, but also because of the significant distortion that occurs in that unit. Of immediate interest is whether this distortion arises because only 16 electrons are available in this case for cluster bonding (6.3 − 10.1 + 8). Eighteen cluster-based electrons appear to be an optimal complement for octahedral clusters centered by a d-element interstitial Z, corresponding to population of the M–Z bonding $a_{1g}^2\ t_{2g}^6$, the M_6 cluster-bonding t_{1u}^6, and the nominally nonbonding e_g^4 orbital on Z.[7] Zirconium iodide clusters centered by 3d elements appear to adhere to this 18-electron minimum quite well, but several rare-earth metal examples in $R_7I_{12}Z$ structures are known with only 16 or 17 electrons, e.g., $Pr_7I_{12}Mn$ and $Pr_7I_{12}Fe$, respectively, perhaps because the t_{1u} HOMO on the more electropositive cluster elements is higher lying relative to the interstitial orbitals.[13] The clusters in all of these have $\bar{3}$ (S_6) symmetry when intercluster connections are included, and the 17-electron $Y_7I_{12}Fe$ shows only a small (0.08 Å, 2.2%) compression of the yttrium trigonal antiprism. Thus, no "electronic" distortions have been observed before although the loss of the center of symmetry has been found in the analogous 13-electron $Sc[Sc_6(Br,I)_{12}C]$.[16]

Figure 3 shows a single 16-electron cluster in $Y_6I_{10}Ru$ together with important Y–Ru and Y–Y distances (the orientation is the same as in Figure 2). A notable cluster distortion is manifest in the unequal Y–Ru distances. The cluster may be roughly described as having undergone a 0.2-Å tetragonal compression along a "4-fold axis" to produce Y2–Ru distances of 2.556 (3) Å relative to the 2.762 (3) Å average for those normal to this pseudoaxis (the cluster possesses only an inversion center). The different modes of iodine bridging represented in Figures 1 and 2 are presumably responsible for the more modest distortion of the Y_6Ru unit from the ideal D_{4h}; the Y–Ru–Y angles deviate from 90° by 2.5° or less while the Y–Y edges of the cluster range from 3.84 Å to 3.97 Å around the waist and from 3.69 to 3.85 Å to Y2 where the compression occurs.

The observed Y–Ru distances indicate a strong bonding interaction, one that is presumably somewhat like but significantly greater than the extended interactions present in Y–Ru intermetallic phases. Thus, the average Y–Ru distance in the cluster, 2.69 Å, compares with 2.86 Å for $\bar{d}$(Y–Ru) in the approximately trigonal-prismatic environment about ruthenium in Y_5Ru_2.[17] (Values in the latter, 2.76–2.98 Å, were calculated by using the refined coordinates for Dy_5Ru_2. A comparable calculation for Y_3Ru using the positional data for Sm_3Ir[18] gives a very similar 2.85-Å value for $\bar{d}$(Y–Ru).) The 0.17-Å shortening of typical intermetallic distances found on cluster formation continues a trend already noted for Sc–Co,[13] Zr–Fe,[7] and Zr–Si[4] separations in analogous $M_6I_{12}Z$-type clusters relative to the corresponding binary phases. The effective oxidation of the condensed cluster unit in the intermetallic phase on formation of these isolated cluster halides may have the general effect of reducing the shielding between the interstitial and the cluster metal, thus allowing a smaller separation. On the other hand, extended Hückel (EH) calculations performed on Zr_3Fe and $Zr_6I_{14}Fe$ indicate[7] that the Zr–Fe bonding is considerably stronger in these cluster compounds as a result of the particulars of the cluster's electronic structure (vide infra). These explanations can be viewed as distinct since the EH method cannot model "shielding" effects.

Calculations. We carried out extended Hückel calculations on this system in an effort to discover whether the distortion of the Y_6Ru octahedron in $Y_6I_{10}Ru$ shown in Figure 3 may derive from, or is consistent with, its "electron deficient" (16-electron) nature. Structural parameters were taken from the X-ray structure determination. Calculations were carried out with a coordinate system rotated such that the z axis was colinear with the short Y2–Ru bonds and two longer Ru–Y bonds were aligned with the x and y axes as closely as the small deviations of the Y–Ru–Y angles from 90° would permit. H_{ii} values used for both yttrium and ruthenium were obtained from a full charge-iterative calculation in which orbital energy parameters for both atoms were allowed to vary simultaneously as a function of Mulliken charge transfer.

To put the problem in perspective, it should be noted that the observed "tetragonal" compression of the Y_6Ru cluster initially seemed surprising since calculations unambiguously show that the HOMO for 18-electron octahedral clusters centered by transition metals has t_{1u} symmetry.[7] Such a compression would normally split the t_{1u} orbital into a one-below-two orbital pattern if Ru 5p contributions are controlling, stabilizing $t_{1u}(z)$ while destabilizing the $t_{1u}(x,y)$ components. These interactions are clearly not optimal to drive the distortion of the 16-electron cluster (unless there is some special stability associated with a triplet state).

In presenting the results of the band structure calculations, we will make use of a level diagram obtained from a calculation for $\vec{k} = 0$ since this will allow us to speak of "molecular orbitals" in this quasi-molecular system. A more extensive band calculation carried out at 32 $\vec{k}$ points in the appropriate triclinic Brillouin zone showed that this is a very good approximation for at least the metal-based orbitals; the metal bands are very narrow and peaked about the energies of the "molecular" orbitals. In other words, the intercluster interactions, either through-space or through-bond, are minor perturbations on the isolated clusters. Of course, all of the exo iodine atoms bonded at the yttrium vertices must still be included in the model for good results.[3] The discussion that ensues also treats the clusters as if they had tetragonal symmetry, and the computational results are for the most part consonant with this point of view. Mixing between levels marked as "t_{2g}" + "a_{1g}" in fact reflects the true C_i symmetry, but this mixing is only appreciable because of the near (accidental) degeneracy of the levels (in O_h symmetry) for this system. As will be evident, these minor perturbations to the overriding tetragonal component of the distortion are not significant.

The calculated splitting pattern shown in Figure 4 reveals that our naive expectations were incorrect and that a two-below-one pattern emerges instead, consonant with the observed structural

(16) Dudis, D. S.; Corbett, J. D.; Hwu, S.-J. *Inorg. Chem.* **1986**, *25*, 3434.

(17) Cenzual, K.; Palenzona, A.; Parthé, E. *Acta Crystallogr.* **1980**, *B36*, 1631.

(18) Le Roy, J.; Moreau, J.-M.; Paccard, D.; Parthé, E. *Acta Crystallogr.* **1979**, *B35*, 1437.

(19) d–dπ and d–dσ overlaps are comparable in this situation. For a fuller discussion of relevant overlaps, see: Burdett, J. K.; Hughbanks, T. *J. Am. Chem. Soc.* **1984**, *106*, 3101.

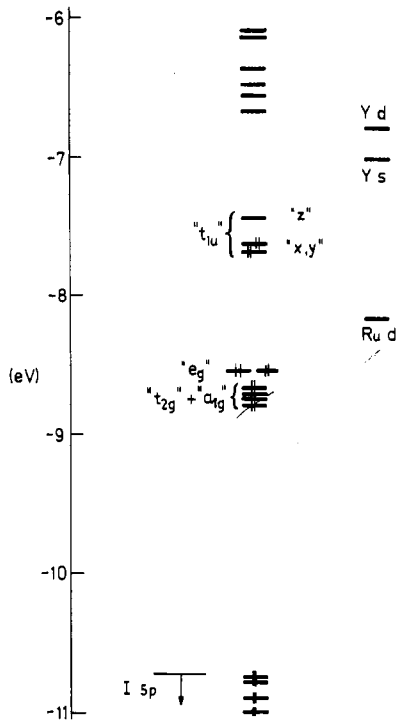

Figure 4. MO levels calculated for the $(Y_6I_{12}Ru)I_6^{8-}$ cluster with the dimensions observed in $Y_6I_{10}Ru$. The "representations" assigned to cluster bonding levels are those for octahedral symmetry. Iodine p bonding and nonbonding levels lie below −10.73 eV, and antibonding cluster levels lie above −6.66 eV.

distortion. This is because the Ru 5p levels lie relatively high (−2.61 eV), which leads to relatively minor mixing of Ru 5p into this MO and a splitting that is determined by Y–Y interactions, as follows.

As shown in **1a**, the tetragonal compression moves the axial yttrium atoms toward the basal yttrium atoms while moving the latter apart. The orbital contributions to the $t_{1u}(z)$ component

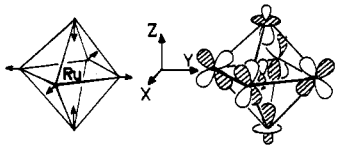

1

(**1b**) show why this member of the t_{1u} set is *destabilized*. First, although the apical–basal distance is shortened in the distortion, the lobes of the d orbitals on the basal atoms move toward the *nodes* of the d_{z^2}-like hybrid on the apical centers, so that the net basal–apical atom overlap in this orbital is relatively small and changes little upon distortion. On the other hand, the concomitant increase in the distances between basal yttrium atoms reduces the d–dπ bonding between these centers[17] and is therefore controlling. The same factors that work to destabilize $t_{1u}(z)$ tend to stabilize $t_{1u}(x,y)$. The insignificance of the high-lying ruthenium 5p orbitals is further demonstrated by removing them from the calculation altogether, whereupon the average splitting between the $t_{1u}(z)$ and the $t_{1u}(x,y)$ components changes by only ~0.02 eV.

Structural Effects. Considerations of possible reasons for the adoption of the $Y_6I_{10}Ru$ structure bring forward again the apparent importance of matrix (closed-shell repulsion) effects. It was noted early that although $Y_7I_{12}Fe$ has been made and characterized structurally, $Y_6I_{10}Fe$ has not been obtained in spite of several attempts to prepare it. On the other hand, the corresponding $Y_7I_{12}Ru$ appears to have limited thermodynamic or kinetic stability with respect to $Y_6I_{10}Ru$ as its yield appears to decrease with increasing temperature or time.

The $Y_7I_{12}Ru$ alternative contains a 17-electron cluster with local D_{3d} symmetry that is, based on the equivalent $Y_7I_{12}Fe$ and other examples, only slightly compressed from a nominal yttrium octahedron. Its disproportionation to the 16-electron $Y_6I_{10}Ru$ affords a structure in which the pseudo-D_{4h} cluster can exhibit axial Y–Ru distances that are significantly shorter than the rest. The capacity to undergo a presumably favorable distortion and still retain reasonable $Y–I^{a-i}$ intercluster (exo) bonding may be important factors in the stability of this structure. As has been noted before,[4,7,13] the minimum lengths found for these exo bonds, especially with iodides, appear to be largely limited by closed-shell contacts the I^a ligand makes with the four adjacent edge-bridging iodines, e.g., 13^a relative to I1, I3, I4, and I5 in Figure 1. Accordingly, $R–I^a$ distances are observed to *decrease* as the size of the interstitial increases since the latter change forces the metal vertices closer to the planes defined at each by neighboring I^i atoms. In this sense the I_{12} cuboctahedron of the cluster can be viewed as somewhat fixed in space while the R_6Z unit moves within it largely in response to the size of Z (and R). (This is not precisely true, since I–I distances are somewhat less in the more condensed ruthenium phase.)

Our convenient reference here is $Y_7I_{12}Fe$ where the $I^a–I^i$ distances are all in the range of 4.15–4.20 Å and $d(Y–I^a)$ is 3.32 Å. The latter distance is presumably somewhat less because of the larger interstitial in $Y_7I_{12}Ru$, while the corresponding $Y_6I_{10}Fe$ is unknown. The average Y–Ru distance in $Y_6I_{10}Ru$ is 0.07 Å greater than Y–Fe in its cluster, which appears to be sufficient to allow tetragonal contraction of the ruthenium cluster to take place with no loss of terminal bond strength. In fact, the $Y1–I2^a$ and $Y3–I5^a$ distances at the "normal" vertices are appropriately reduced to 3.22 and 3.24 Å in $Y_6I_{10}Ru$ while $I^i–I^a$ contacts at both are marginally larger, 4.20–4.23 Å except for one at 4.16 Å. More importantly, the $Y2–I3^a$ distance at the contracted vertex is still as short as it was in $Y_7I_{12}Fe$ (above), and the $I^i–I^a$ contacts thereabout are also the same range. This inferential argument suggests that it may be primarily these subtle bonding factors in the presence of the larger interstitial that allow such a distortion in the novel $Y_6I_{10}Ru$. The inferior $Zr–I^a$ bonding that is achieved with smaller cluster metal atoms in $Cs_xZr_6I_{14}Fe$ and the like is very evident.[3,7]

While zirconium cluster phases containing larger 4d or 5d interstitials have not yet been found, $Y_6I_{10}Z$ phases are stable with a surprising variety of platinum metals in the interstitial Z function.[20] Further characterization of these will doubtlessly reveal more of the diverse factors that go into the bonding and stability of these novel cluster phases.

Acknowledgment. The synthetic and structural portions of this research were supported by the National Science Foundation, Solid-State Chemistry, via Grant DMR-8318616, and were performed in facilities of Ames Laboratory, DOE. The MO calculations were carried out at Texas A&M with the support of the Welch Foundation.

Supplementary Material Available: Tables of refined anisotropic thermal parameters and extended Hückel parameters for $Y_6I_{10}Ru$ and crystallographic details (3 pages); tables of observed and calculated structure factors for $Y_6I_{10}Ru$ (5 pages). Ordering information is given on any current masthead page.

(20) Payne, M. W.; Corbett, J. D. Unpublished research.